Brazilian Journal of Geology

Fonte: http://www.scielo.br/scielo.php?script=sci_arttext&pid=S2317-48892015000200293&lng=en&nrm=iso. Acesso em: 19 mar. 2018.

REFERÊNCIA

SOUZA, Valmir da Silva et al. K'Mudku A-type magmatism in the southernmost Guyana Shield, central-north Amazon Craton (Brazil): the case of Pedra do Gavião syenogranite. **Brazilian Journal of Geology,** São Paulo, v. 45, n. 2, p. 293-306, abr./jun. 2015. Disponível em: <http://www.scielo.br/scielo.php?script=sci_arttext&pid=S2317-48892015000200293&lng=en&nrm=iso>. Acesso em: 19 mar. 2018. doi: http://dx.doi.org/10.1590/23174889201500020008.

DOI: 10.1590/2317488920150002008

ARTICLE

K´Mudku A-type magmatism in the southernmost Guyana Shield, central-north Amazon Craton (Brazil): the case of Pedra do Gavião syenogranite

Magmatismo K´Mudku do tipo A no extremo sul do Escudo das Guianas, centro-norte do Craton Amazonas (Brasil): o caso do sienogranito Pedra do Gavião.

Valmir da Silva Souza[1]*, Antônio Gilmar Honorato de Souza[2], Elton Luiz Dantas[1], Cristóvão da Silva Valério[3]

ABSTRACT: The Mesoproterozoic K'Mudku event (1490 – 1147 Ma) is represented by a britlle-ductile shear belt that cuts across the Paleoproterozoic units in the southernmost Guyana shield, central-north Amazon craton. This event produced mylonitization and cataclasites at low/medium- to high-grade metamorphic, and local within-plate magmatism. In the Amazonas State, Brazil, A-type magmatism chronologically associated to K'Mudku has been reported for the Pedra do Gavião and Samaúma syenogranites. However, the spatial relationship between K´Mudku event and A-type magma generation are not yet adequately clarified in the region. The Pedra do Gavião syenogranite is a high-K alkaline, metaluminous, reduced A-type granite with a post-collisional to within-plate geochemical signature. It has U-Pb zircons crystallization age of 1218 Ma and inherited zircons with ages between 1820 and 1720 Ma, which, together with the Sm-Nd data, suggest melting of Paleoproterozoic basement rocks of the Cauaburi Complex (1810 – 1780 Ma) regional unit. These data demonstrate that the effects of the A-type magmatism associated to the end of the Grenvillian-Sunsas orogeny, reported primarily in the southwestern margin of the Amazon craton, may also be extended for the central-northern part of the Amazon craton. Probably the generation or emplacement mechanisms of A-type magma occurred with some degree of involvement in the final stages of the K´Mudku event. However, this tectonic framework conception still needs more geological and geophysical investigations. Therefore, these news data should instigate to the return of geological research in the region, as well as to debate on the tectonic evolution and A-type granites production during the Ectasian-Stenian period in the central-north Amazon craton.

KEYWORDS: Guyana shield; Amazon craton; K'Mudku event; A-type magmatism; Amazonas State.

RESUMO: *O evento mesoproterozoic K´Mudku (1490 – 1147 Ma) é representado por um cinturão de cisalhamento rúptil-dúctil que atravessa unidades paleoproterozóicas no sul do Escudo das Guyanas, centro-norte do craton Amazonas. Esse evento produziu milonitização e cataclasitos em baixo a alto grau metamórfico com geração localizada de magmatismo intraplaca. No Estado do Amazonas, magamatismo do tipo A cronologicamente associado ao K´mudku tem sido reportado pelos sienogranitos Samaúma e Pedra do Gavião. Entretanto, a relação espacial o evento K´Mudku e a geração de granitos do tipo A ainda não está esclarecida na região. O sienogranito Pedra do Gavião tem assinatura geoquímica alcalina de alto K_2O, metaluminoso, tipo A reduzido e intraplaca a pós-colisional. Tem idade de cristalização U-Pb 1218 Ma e herança entre 1820 e 1720 Ma, que juntamente com os dados Sm-Nd, sugerem fusão de rochas do embasamento paleoproterozóico associadas à unidade regional Complexo Cauaburi (1810 – 1780 Ma). Esses dados demonstram que os efeitos do magmatismo do tipo A associado ao final da orogenia Grenvilliana-Sunsás, relatado principalmente na borda sudoeste do craton Amazonas, pode ser também estendido para a parte centro-norte do craton Amazonas. Provavelmente, os mecanismos de geração ou emplacamento de magmas do tipo A ocorreu com algum grau de envolvimento nos estágios tarde a pós do evento K´Mudku. Contudo, a concepção desse quadro tectônico ainda carece de mais informações geológicas e geofísicas. Portanto, esses novos dados devem instigar ao retorno dos trabalhos geológicos na região, bem como ao debate sobre a evolução tectônica e produção de granitos tipo A durante período Ectasiano-Steniano no centro-norte do craton Amazonas.*

PALAVRAS-CHAVE: *Escudo das Guianas; craton Amazônico; evento K´Mudku; magmatismo do tipo A; Estado do Amazonas.*

[1]Geosciences Institute, Universidade de Brasília – IG-UnB, Brasília (DF), Brazil. *E-mails: vsouza@unb.br; elton@unb.br*

[2]Geological Survey of Brazil – CPRM, Manaus (AM), Brazil. *E-mail: gilmar.souza@cprm.gov.br*

[3]Geosciences Institute, Universidade Federal de Roraima – UFRR, Boa Vista (RR), Brazil. *E-mail: cristovao.valerio@ufrr.br*

*Corresponding author

Manuscrito ID: 30209. **Received:** 11/24/2014. **Approved:** 04/28/2015.

INTRODUCTION

The southernmost Guyana shield, in the central-north Amazon craton, comprises different Paleoproterozoic geotectonic provinces amalgamated during successive episodes of microcontinent–continent collisions. In Brazil, the names, geographic boundaries and age intervals of these geotectonic provinces are still controversial issues (*e.g.,* Tassinari & Macambira 1999, Tassinari *et al.* 2000, Santos *et al.* 2000, 2006a, Santos 2003). This region also comprises a Mesoproterozoic event named K'Mudku (1.49 – 1.14 Ga), which is a brittle-ductile sinistral shear belt of SW-NE direction that cuts across the Paleoproterozoic geotectonic units (Fig. 1A). The K´Mudku event produced mylonitization and cataclasites, marked by several pulses resetting K-Ar and Rb-Sr isotopic systems of Paleoproterozoic units and local rock melting (Barron 1966, Priem *et al.* 1971, Bosma *et al.* 1983, Gibbs & Barron 1993, Fraga & Reis 1996, Santos *et al.* 2000, 2008, Fraga 2002, Fraga *et al.* 2009, Cordani *et al.* 2010). This event has been considered to be a structural far-field effect of the Grenvillian-Sunsas orogenies affecting the central-north part of the Amazon craton associated to an intracratonic tectonic setting (Teixeira 1978, Santos *et al.* 2000, 2006b, 2008, Cordani *et al.* 2010).

On the other hand, during the last ten years, an increasing number of geological and geochronological studies in this region recognized the effects of the K´Mudku event also outside the limits of shear belt, especially regarding the A-type magmatism generation (Santos *et al.* 2006b, 2009, Souza *et al.* 2006). Although Mesoproterozoic (1.55 – 1.54 Ga) A-type magmatic units are known since the 1970s in the southernmost Guyana shield, especially in the State of Roraima, such as the Surucucus and Mucajaí intrusive suites (Montalvão *et al.* 1975, Gaudette *et al.* 1996, CPRM 1999, Fraga et al. 2009, Almeida *et al.* 2003). Records of Mesoproterozoic A-type magmatism chronologically associated to K´Mudku deformational event leads to the debate on the tectonic evolution in the central-north Amazon craton, emphasizing the geological/tectonic events responsible for the generation of A-type granites during the Ectasian-Stenian period.

In this paper we present new petrographic, geochemical and geochronological (U-Pb and Sm-Nd) data for the Pedra do Gavião A-type syenogranite located in the Amazonas state, in order to understand the nature of the Mesoproterozoic A-type magmatism chronologically related to the K'Mudku event in the southernmost Guyana shield.

ANALYTICAL PROCEDURES

The petrographic investigations and modal analyses on eight rock samples were undertaken at the microscopy laboratory of the University of Brasília. The samples were chosen and prepared applying crushing and pulverizing in an agate shatter box at the isotope geology laboratories of the University of Brasília for geochemistry and Sm-Nd isotopic analyses. Whole-rock powders (ca. 10 mg) geochemical analyses were carried out at ACME Analytical Laboratories Ltd., Vancouver, Canada. The samples were analyzed for major elements (SiO_2, TiO_2, Al_2O_3, Fe_2O_{3tot}, MnO, MgO, CaO, Na_2O, K_2O, and P_2O_5) by Inductively Coupled Plasma-Emission Spectrometry (ICP-ES) and for trace and rare-earth elements by Inductively Coupled Plasma-Mass Spectrometry (ICP-MS).

The isotopic analyses (U–Pb and Sm–Nd) were carried out at the Isotope Geology laboratories of the University of Brasília, applying the analytical procedures below:

- U–Pb analyses were done by LA-MC-ICP-MS following the analytical procedure described by Bühn *et al.* (2009). Zircon concentrates were extracted using conventional gravimetric and magnetic separation techniques. The zircon grains were selected under a binocular microscope to obtain fractions of similar size, shape and color. For *in situ* U–Pb, hand-picked zircon grains were mounted in epoxy blocks and polished to obtain a smooth surface. Backscattered electron images were obtained in order to investigate the internal structures of the zircon crystals prior to the analysis. The laser microprobe is a New Wave UP213 Nd:YAG laser (λ = 213 nm), connected with a Thermo Finnigan Neptune Multi-collector ICP-MS. Helium was used as the carrier gas and mixed with argon before entering the ICP. The laser was run at a frequency of 10 Hz and energy of ~100 mJ/cm^2 with a spot of 30 µm for U–Pb dating and 40 µm for Hf isotopic analyses. U–Pb diagrams and age calculations were done using ISOPLOT version 3.0 (Ludwig 2003) and errors for isotopic ratios are presented at the 1σ level.
- Sm–Nd isotopic analyses followed the method described by Gioia & Pimentel (2000). Whole rock powders (ca. 50 mg) were mixed with ^{149}Sm-^{150}Nd spike solution and dissolved in Savillex capsules. Sm and Nd extraction of whole-rock samples followed conventional cation exchange techniques, using teflon columns containing LN-Spec resin (HDEHP – diethylhexil phosphoric acid supported on PTFE powder). Sm and Nd samples were loaded on Re evaporation filaments of double filament assemblies and the isotopic measurements were carried out on a multi-collector Finnigan MAT 262 mass spectrometer in static mode. Uncertainties for Sm/Nd and ^{143}Nd/^{144}Nd ratios are better than ± 0.2% (2σ) and ± 0.003% (2σ) respectively, based on repeated analyses of international rock standards BHVO-1 and BCR-1. ^{143}Nd/^{144}Nd ratios were normalized to ^{146}Nd/^{144}Nd of 0.7219 and the decay constant (λ) used was 6.54×10^{-12}/a. Nd T_{DM} values were calculated using De Paolo (1981) model.

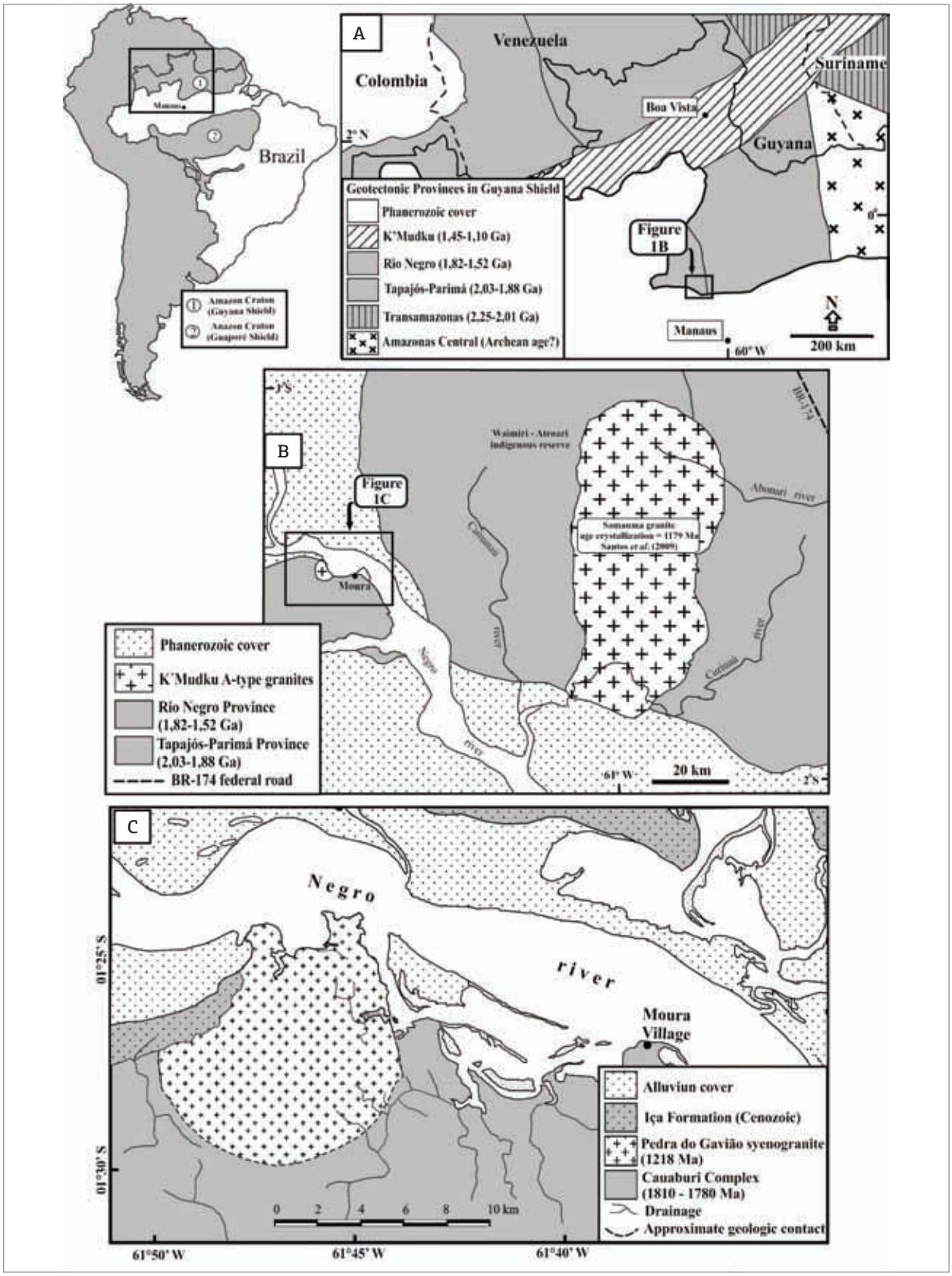

Figure 1. (A) Geotectonic provinces distribution in the central- northern portion of the Amazon craton and location of the study area (modified from Santos *et al.* 2006b); (B) Simplified regional geological map showing the studied area (modified from Santos *et al.* 2009); and (C) Geological map of the area of occurrence of the Pedra do Gravião syenogranite (modified from Souza *et al.* 2006).

GEOLOGICAL SETTING

Different geotectonic models have been put forward over the last decades to explain the evolution of the Amazon craton, mainly based on geochronological data. The two main current evolution models proposed for the Brazilian side of the Amazon craton include the Pedra do Gavião syenogranite into different geotectonic/geochronological provinces: a) the model of Tassinari and Macambira (1999) and Tassinari *et al.* (2000), considers that the Pedra do Gavião syenogranite is part of the Ventuari-Tapajós geotectonic province (1.95 – 1.80 Ga); and b) the model suggested by Santos *et al.* (2000, 2006a) considers it part of the Rio Negro geotectonic province (1.82 – 1.52 Ga) (Fig. 1A).

In this paper we will use the configuration applied for model proposed by Santos (2000, 2006a), simply because it display the distribution of the K'Mudku event on the different geotectonic/geochronological provinces from Amazon craton. Therefore, it is not the objective of this paper to discuss or to support any geotectonic/geochronological model presented for the Amazon craton.

The Paleoproterozoic basement of the Rio Negro geotectonic province is represented by the regional unit named Cauaburi Complex (Lima & Pires 1985), which is composed by arc-type granitoids, meta-granites, gneisses, amphibolites and migmatites deformed in a NE-SW direction. The U-Pb ages of these rocks vary between 1.81 and 1.78 Ga and their Sm/Nd ratios suggest mixing of crust-mantle sources (Santos 2003, CPRM 2006, Santos *et al.* 2006b, Almeida *et al.* 2007, 2013). Additionally, several Mesoproterozoic (1.52 – 1.48 Ga) I-, S- and A-type magmatic suites and mafic-ultramafic units, associated to the Içana orogeny (Almeida *et al.* 2013), occur intrusive in the Paleoproterozoic basement rocks.

During the Mesoproterozoic (1.49 – 1.14 Ga), a wide area involving Venezuela, Guyana and Suriname, as well as all Paleoproterozoic provinces of the southernmost Guyana shield in Brazil were affected by the K'Mudku deformational episode (Fig. 1A). On the Brazilian side, this episode is mainly registered in the Roraima State, within of the Guyana Central belt geological domain (Fraga & Reis 1996). According to Fraga and Reis (1996), Fraga (2002) and Fraga *et al.* (2009), the K´Mudku episode produced a set of brittle-ductile shear zones with NE-SW foliation, as well as contraction and strike-slip faults with cataclasite generation, with partial to total obliteration on to Paleo- to Mesoproterozoic pre-existing structures, developed by a lithospheric transpression mechanism at the low-grade metamorphic conditions. On the other hand, Santos *et al.* (2006b) argue that the K'Mudku episode was a collisional zone active for approximately 300 Ma, which produced sinistral thrusts-shear zone oblique at medium to high-grade metamorphic conditions and occurrence of bimodal magmatism. However, the role of the K'Mudku episode in the geological evolution of the Amazon craton is still poorly understood.

Some A-type granites, located outside of the structural limits of the K´Mudku belt, have been chronologically associated to this K´Mudku event. These are reported by the Saracura granite (1308 Ma) in the Roraima State (Santos *et al.* 2006b, 2009), and by the Samaúma batholith (1179 Ma) and the Pedra do Gavião stock (1218 Ma) in the Amazonas State (Santos *et al.* 1974, 2009, Souza *et al.* 2006). It is probable that this A-type magmatism is a distal representation of the late to post-K´Mudku event, but the tectonic framework and emplacement mechanism are still not understood. Moreover, this region has limited geological information, especially within of the Waimiri-Atroari indigenous reserve (Fig. 1B). It is probable that there are others A-type granitic bodies in the region, which can be parts of an intrusive suite that has not been yet studied adequately.

PEDRA DO GAVIÃO SYENOGRANITE

The Pedra do Gavião syenogranite is exposed on the right bank of the Negro river and about 200 km to the southwest of Manaus city. It has an elliptical shape (*c.* 15 x 10 km), intrusive into rocks of the Cauaburi Complex and is partially covered by the Cenozoic Içа Formation and by alluvial sediments (Fig. 1C). The granite is pink colored, displays inequigranular medium- to coarse-grained texture and isotropic fabric (Fig. 2A and 2B), presents technical characteristics that allow its use as ornamental rock, but it has been mainly used as crushed stone to supply the construction industry (Maas & Souza 2009). It is cut by NNE-SSW discrete normal faults and fractures. It contains amphibolite and gneiss xenoliths from the Cauaburi Complex, ranging in size from a few centimeters to 50 cm, distributed mainly along the boundaries of the granitic body (Fig. 2C).

Petrography

The Pedra do Gavião mineralogy is uniform and dominated by alkali feldspar (microcline, 54 – 62%), followed by quartz (22 – 27%), plagioclase (An_{14-18}, 13 – 15%), amphibole (8 – 11%) and biotite (< 8%). The accessory minerals are sphene, apatite, zircon, allanite, ilmenite, pyrite, sphalerite and traces of chalcopyrite. Chlorite, epidote, white mica, carbonate and Fe-hydroxides are secondary minerals.

The microcline crystals are anhedral to subhedral with grain sizes of 5 – 10 mm. It is strongly microperthitic with stringlets, strings, interlocking and chessboard exsolutions of albite (An_{4-6}) crystals (Fig. 2D), showing slightly undulatory extinction and local inclusions of rounded quartz and

partially altered plagioclase (albite to oligoclase). Quartz and plagioclase occupy interstices between microcline aggregates. Quartz appears as isolated anhedral crystals of 0.5 – 1.5 mm or crystal aggregates, shows slight undulatory extinction and is partially recrystallized. Plagioclase (oligoclase) forms rectangular to subhedral plates of 1 – 2 mm, with albite twinning, oscillatory-zoned portions and variable degrees of substitutions (white mica, ± epidote and carbonate).

Amphibole occurs as subhedral isolated crystals of 0.3 – 0.8 mm or as crystal aggregates associated with biotite. The pleochroism from pale brown to dark-green color suggests that is hastingsite-type amphibole. These crystals are

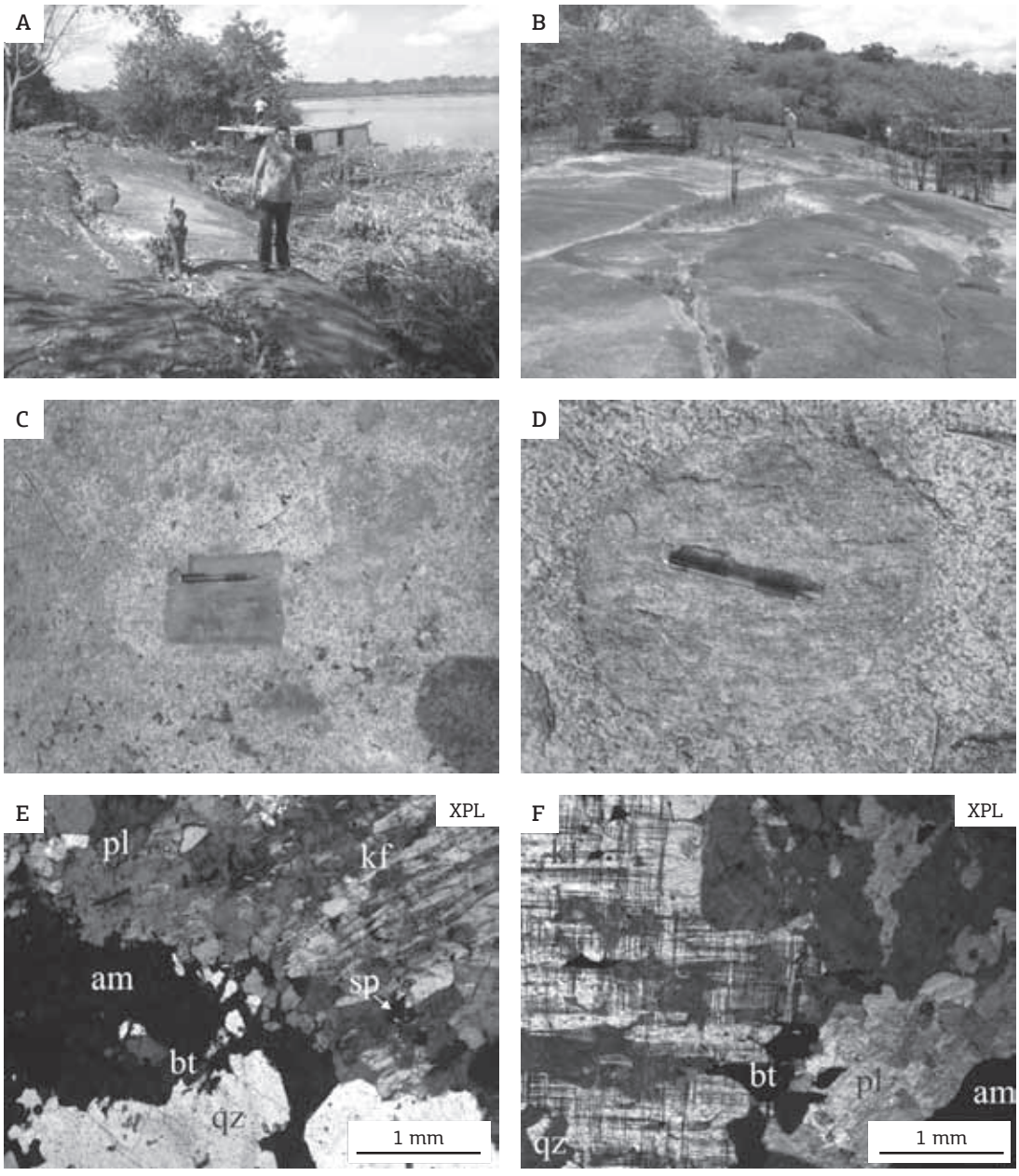

Figure 2. (A) and (B) Outcrop of the Pedra do Gavião syenogranite on the bank of the Negro river; (C) and (D) inequigranular medium- to coarse-grained texture forming an isotropic fabric in the Pedra do Gavião syenogranite with amphibolite and gneisses xenolith fragments; (E) and (F) microtextural relationships of petrographic features. The microcline crystals (kf) are clearly identified by the typical crosshatched twinning and microperthitic texture. Quartz (qz), plagioclase (pl), amphibole (am), biotite (bt) and accessory minerals (*e.g.* sp = sphene) occupy interstices between microcline aggregates (XPL = crossed polarisers).

partially replaced by biotite and chlorite, as well as epidote and Fe-hydroxides. Biotite shows pleochroism from dark brown to green-yellowish flakes and is partially replaced by chlorite and Fe-hydroxides. The accessory mineral phases are generally euhedral to subhedral and usually enclosed in amphibole, biotite and sulfide aggregates. The zircon crystals are notable for its size (up to 500 µm long) and by showing oscillatory zoning.

The mineralogical characteristics of the Pedra do Gavião granite is indicative of A-type magmatism, with high contents of microperthitic alkali feldspar, zoned plagioclase, as well as amphibole and biotite as insterstitial crystals (Collins *et al.* 1982, Clemens *et al.* 1986). On a modal Q-A-P diagram, the mineral proportions allow it to be classified as a biotite-hastingsite syenogranite (Fig. 3).

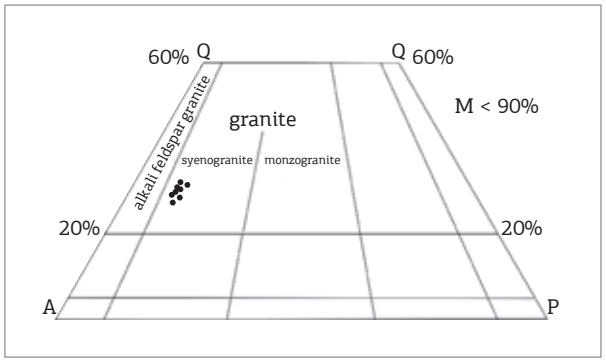

Figure 3. Modal Q-A-P diagram apply for Pedra do Gavião rock samples (Streckeisen 1976).

Whole-rock Geochemistry

Whole-rock chemical compositions of seven samples of the Pedra do Gavião syenogranite are listed in Table 1 and discussed below.

The whole-rock chemistry composition is uniform and marked by limited range of SiO_2 (70 – 72 wt.%), Al_2O_3 (~13 wt.%), K_2O (~6 wt.%), FeO_t (~3.1 wt.%), Na_2O (~3.5 wt.%), CaO (~1 wt.%), TiO_2, MnO, MgO, P_2O_5 and LOI (< 0.5 wt.%). These rocks have high-alkalis contents (K_2O + Na_2O = 9.34 – 9.82 wt.%) that indicate an alkaline composition with high-K. This can be shown on the Na_2O + K_2O – CaO *versus* SiO_2 diagram with samples concentrated in the alkalic field (Fig. 4A). On the aluminum saturation index (ASI, from Shand 1943) and represented by A/NK *versus* A/CNK diagram, the samples plot in the metaluminous field (Fig. 4B). Additionally, on the CaO/(FeOt+MgO+TiO_2) *versus* CaO+Al_2O_3 diagram, the samples plot in the A-type field (Fig. 4C) and on FeOt/(FeOt + MgO) *versus* SiO_2 diagram, the samples plot in ferroan A-type granitoids field (Fig. 4D). According to Frost *et al.* (2001a), ferroan A-type granitoids reflect a close affinity anhydrous, alkalic and reduced magmas common in extensional environments, generally hotter and likely to undergo extensive fractionation process.

The Pedra do Gavião syenogranite is relatively enriched in Ba, Co, Hf, Ga, Nb, Rb, Th, Y, Zr and Ce. The multi-elements diagram indicates typical compositions of upper continental crust rocks, marked by positive Rb, Th, K, La, Ce, Nd and Zr anomalies and negative Ba, Nb, Ta, Sr, and Ti anomalies (Fig. 5A) (*e.g.* Thompson 1982, Rollinson 1993). Chondrite-normalised rare earth element (REE) distribution patterns are presented in the Figure 5B. It is enriched in light rare earth elements (LREE) and relatively depleted in heavy rare earth elements (HREE). La+Ce vary between 120 and 140 ppm and Tm+Yb is in the range 20 – 30 ppm. The REE contents display strong fractionation of the LREE group with $(La/Sm)_N$ between 5.45 – 4.15 and a flat pattern of the HREE group with $(Gd/Yb)_N$ of 1.33 – 1.36, separated by pronounced negative Eu anomalies (Eu/Eu* = 0.22 – 0.26).

The Pedra do Gavião syenogranite presents geochemical characteristics typicals of A-type granites, such as high contents of alkalis (K_2O + Na_2O), Zr, Ce, Ba, HREE and 10^4Ga/Al ratios of 2.85 – 3.29, and low contents of CaO, MgO, P_2O_5, TiO_2, Sr and Eu (Table 1) (*e.g.* Collins *et al.* 1982, Clemens *et al.* 1986, Whalen *et al.* 1987, Eby 1990, 1992). On the Zr+Nb+Ce+Y *versus* 10^4Ga/Al diagram, the samples plot in the A-type granites field (Fig. 6A), and on FeOt/(FeOt+MgO) *versus* Al_2O_3 diagram, the samples plot in the reduced A-type granites field (Fig. 6B), suggesting derivation from quartz-feldspathic igneous sources (Dall´Agnol & Oliveira 2007). Additionally, on the ternary diagram Nb–Y–3Ga, the samples plot in the A_2-subtype field with Y/Nb ratios > 1.2 (Fig. 6C), indicating emplacement during extensional collapse of an orogenic belt (Eby 1992). Finally, on the Rb *versus* Y+Nb diagram, the samples plot in the post-collisional to within-plate fields (Fig. 5D).

Geochronological data (U-Pb and Sm-Nd)

U-Pb and Sm-Nd data for samples from Pedra do Gavião syenogranite are listed in Tables 2 and 3, and are discussed below.

For the U-Pb analyses, the GH-1 rock sample was chosen and a total of 22 zircon crystals were selected for analyses. Two populations of zircon crystals were identified in the sample. The first population (type 1) comprises pale yellow to pale pink, but with rare colorless, long-prismatic euhedral to subhedral crystals (180 – 260 µm). They present few micro-inclusions and micro-fractures, and some crystals are slightly zoned. The second population (type 2) is formed by pale brown to brown short-prismatic subhedral crystals (80 – 160 µm), which are zoned or have inherited cores with several micro-inclusions and some micro-fractures.

Table 1. Whole-rock geochemical compositions of the Pedra do Gavião syenogranite.

Sample	GH-5b	GH-5c	GH-6	GH-5	GH-4b	GH-4	GH-2
SiO_2 (%)	71.08	70.69	72.33	71.88	70.68	71.39	70.85
TiO_2	0.44	0.38	0.41	0.41	0.39	0.38	0.40
Al_2O_3	13.26	13.52	13.31	13.14	13.77	13.64	13.76
FeOt	3.15	3.15	2.81	3.32	3.20	3.10	3.14
MnO	0.08	0.08	0.07	0.07	0.06	0.06	0.07
MgO	0.17	0.07	0.08	0.15	0.09	0.09	0.15
CaO	1	0.99	0.94	1.03	1.02	0.99	1.11
NaO_2	3.41	3.52	3.54	3.42	3.63	3.56	3.67
K_2O	5.94	6.04	6.01	5.92	6.16	6.26	6.05
P_2O_5	0.14	0.06	0.04	0.06	0.05	0.04	0.05
LOI	0.80	0.80	0.20	0.30	0.40	0.20	0.40
total	99.47	99.30	99.74	99.70	99.45	99.51	99.65
Ba (ppm)	419	433	351	430	382	388	362
Be	3	4	3	3	3	3	3
Co	61	64	62	65	72	68	66
Cs	2.8	3.2	3.5	3.5	2.6	2.6	3.5
Cu	2	2	2	2	2	3	2
Ga	20	21	21	22	24	23	22
Hf	26.5	16.6	16.3	20.6	17.8	19.5	22
Mo	1.4	1.4	2	2	3	3.87	1.7
Nb	30.7	28.3	25	28.2	18.9	18.7	28.1
Pb	13	14	16	13	17	18	18
Rb	193	204	216	212	227	231	230
Sc	6	5	4	6	5	5	5
Sn	4	4	3	3	3	3	3
Sr	55	58	47	53	48	50	51
Ta	1.7	1.5	1.8	1.8	1.5	1.6	2
Th	23.4	21.9	20.5	22.8	25.2	26.7	22.6
U	5.7	5.5	6.9	5.5	5.4	5.5	6.7
W	3.5	3.7	2.8	2.6	3	2.8	3.2
Y	60	59	63	69	77	77	72
Zn	57	60	55	71	71	72	60
Zr	1026	645	589	725	668	720	762
La (ppm)	95	96.1	115	113.5	157	155.5	98.4
Ce	205.1	202.3	244.7	250.6	325.4	318.2	213.7
Pr	22.97	22.82	25.26	25.73	32.09	31.84	22.55
Nb	86.1	88.3	95.5	99.6	122.1	117.6	90.5
Sm	14.3	14.43	15.7	16.2	18.7	18.9	15.5
Eu	1.12	1.13	1.17	1.28	1.27	1.21	1.19
Ga	11.31	11.32	12.06	11.61	13.88	14.4	12.07
Tb	1.95	1.92	2.01	2.11	2.46	2.33	2.22
Dy	10.77	10.46	10.8	12.3	14.06	13.4	12.06
Ho	2.16	2.12	2.32	2.43	2.62	2.56	2.47
Er	6.61	6.3	6.32	7.08	7.92	7.67	7.41
Tm	1.05	1	1.03	1.15	1.21	1.17	1.21
Yb	6.85	6.4	6.4	7.16	7.6	7.06	7
Lu	1.1	1.06	1.05	1.18	1.27	1.29	1.17
K_2O+Na_2O	9.35	9.56	9.55	9.34	9.79	9.82	9.72
K_2O+Na_2O-CaO	8.35	8.57	8.61	8.31	8.77	8.83	8.61
FeOt/(FeOt+MgO)	0.94	0.94	0.97	0.95	0.97	0.97	0.95
CaO/FeOt+MgO+TiO_2	0.26	0.27	0.28	0.26	0.27	0.27	0.30
CaO+Al_2O_3	14.26	14.41	14.25	14.17	14.79	14.63	14.87
Y+Nb	90.7	87.3	88	97.2	95.9	95.7	100.1
$(La/Sm)_N$	4.18	4.19	4.63	4.40	5.45	5.21	4.15
$(Gd/Yb)_N$	1.33	1.36	1.32	1.39	1.33	1.39	1.34
$(Eu/Eu^*)_N$	0.26	0.26	0.25	0.28	0.24	0.22	0.26
10^4Ga/Al	2.85	2.93	2.98	3.16	3.29	3.18	3.04
Zr+Nb+Ce+Y	1321.8	934.6	921.7	1072.8	1089.3	1133.9	1075.8

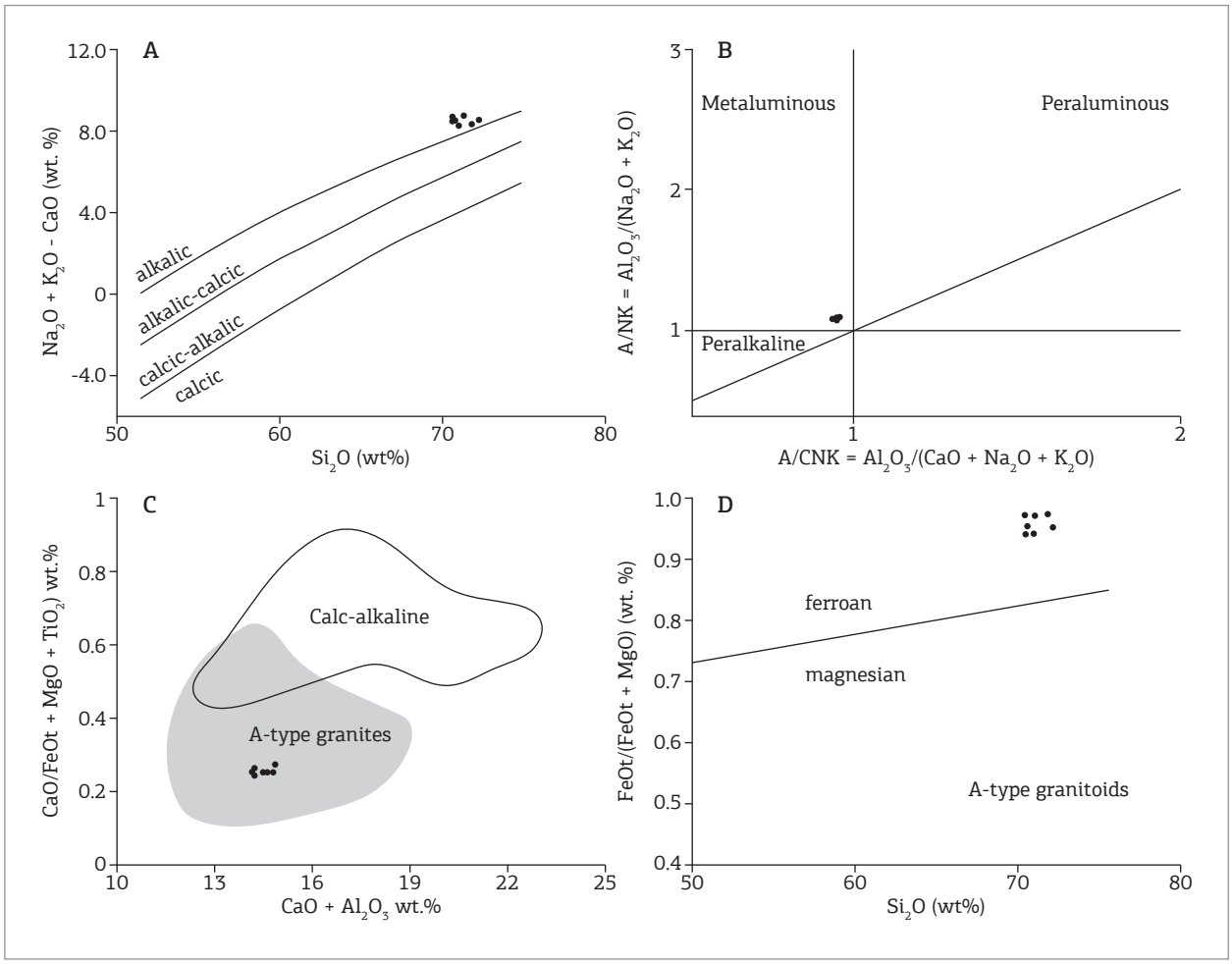

Figure 4. Geochemical diagrams apply for rocks of the Pedra do Gavião syenogranite. (A) Modified alkali-lime index diagram MALI = Na_2O + K_2O - CaO *versus* SiO_2 (Frost *et al.* 2001a); (B) Aluminum saturation index (ASI total) diagram (Maniar & Piccoli 1989); (C) CaO/(FeOt+MgO+TiO_2) *versus* CaO+Al_2O_3 diagram to distinguish A-type and calc-alkaline granites (Dall´Agnoll & Oliveira 2007); (D) FeOt/(FeOt + MgO) *versus* SiO_2 diagram applied to distinguish between ferroan and magnesian A-type granitoids (Frost *et al.* 2001a).

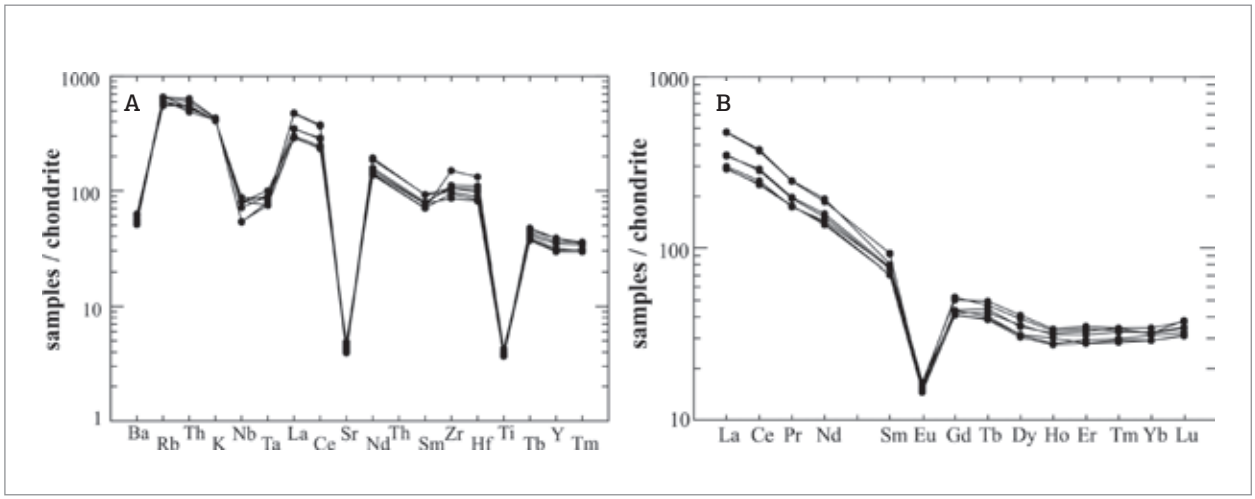

Figure 5. (A) and (B) Multi-elements and REE distribution patterns. Values are normalized according to Thompson (1982) primordial mantle and Boynton (1984) chondritic values.

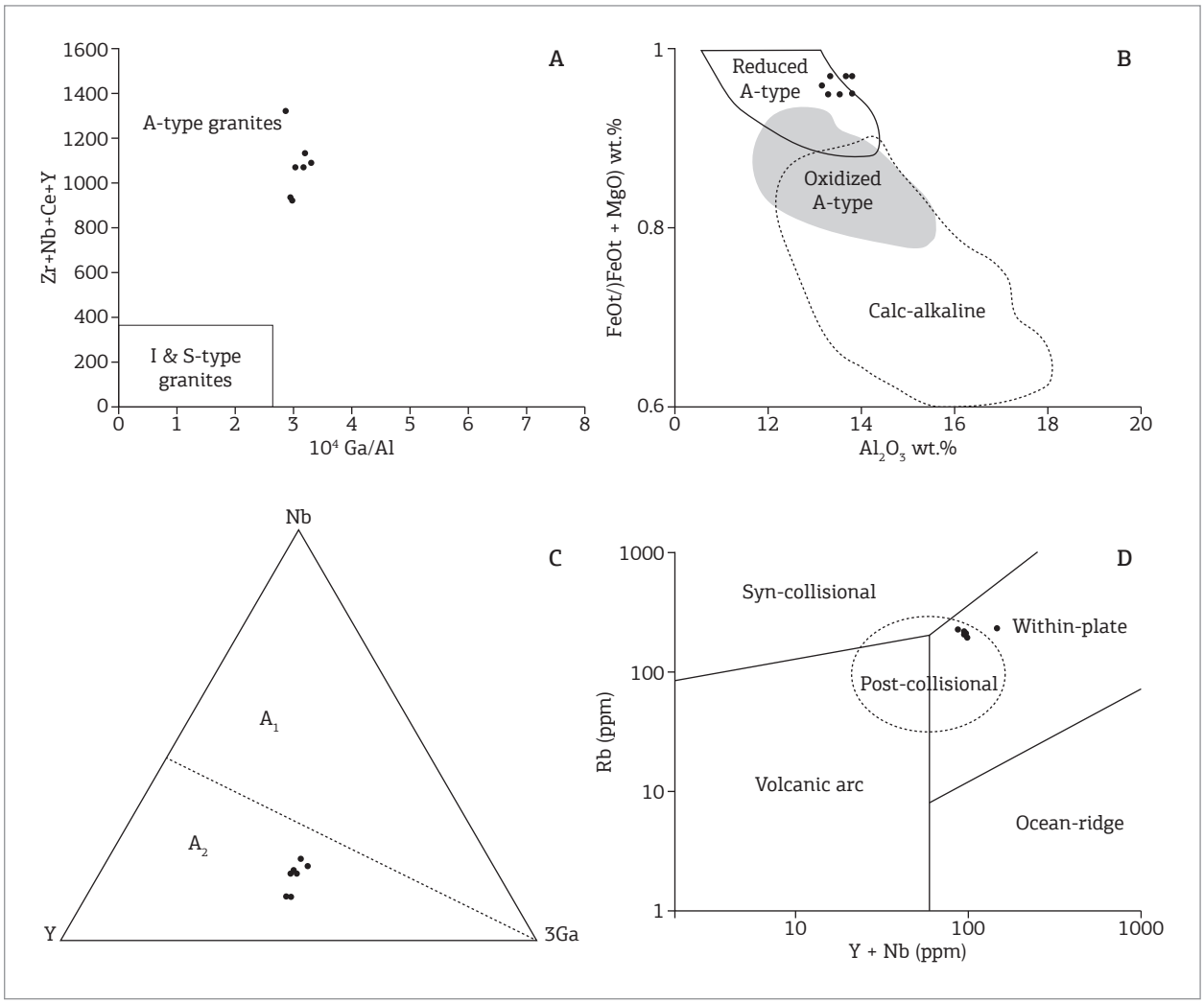

Figure 6. Discrimination diagrams applied to the Pedra do Gavião syenogranite. (A) Zr+Nb+Ce+Y *versus* 10^4Ga/Al diagram applied to distinguish A-type granites (Whalen *et al.* 1987); (B) FeOt/(FeOt+MgO) *versus* Al_2O_3 diagram, separating A-type and calc-alkaline granite fields (Dall´Agnol & Oliveira 2007); (C) Nb-Y-3Ga triangular diagram distinguishing between A_1 and A_2 granitoids (Eby 1992); and (D) Rb *versus* Y + Nb tectonic setting diagram (Pearce *et al.* 1984).

Six to seven crystals of type 1 zircon yielded U-Pb isotopic ratios indicating a concordia age of 1218 ± 5 Ma, which is interpreted as the crystallization age of the Pedra do Gavião syenogranite (Fig. 7). This is in agreement with the crystallization age of 1231 ± 5 Ma reported by Souza *et al.* (2006) using the ID-TIMS U-Pb method of a similar rock from the same intrusion. On the other hand, it appears that type 2 population, with ages between 1820 – 1720 Ma (Fig. 7), are indicating inheritance ages from the Paleoproterozoic basement Cauaburi Complex (1810 – 1780 Ma; Almeida *et al.* 2007, 2013).

Whole-rock Sm–Nd analyses were performed on four selected rock samples (Tab. 3 and Fig. 8). Samples GH-04, GH-06 and GH-11 presented negative εNd(t = 1,218) values ranging from -3.09 to -4.22, Nd T_{DM} model age from 1.76 to 1.86 Ga, and fractionation factor (*f* Sm/Nd) between -0.48 and -0.50, calculated using the equation of Goldstein *et al.* (1984). In general, these values are typical of crustal sources generated in the late Paleoproterozoic, during the Statherian period. On the other hand, the sample GH-02 presented a high $^{147}Sm/^{144}Nd$ ratio of 0.1560, εNd(t = 1218) of -9.98, Nd T_{DM} model = 3.34 Ga and *f* Sm/Nd = -0.20, probably reflecting the anomalously high amount of alkali feldspar in the rock.

DISCUSSION

Increasing evidence of A-type magmatism chronologically related to the Mesoproterozoic K'Mudku (1490 – 1147 Ma) event in the southernmost Guyana shield have been recently reported in the literature, especially in Roraima and Amazonas states. In general, these K´Mudku A-type granites have texture, petrographic and geochemical features similar to those of the Paleopreoterozoic Mapuera and Madeira A-type

Table 2. U-Pb isotopic data for zircon crystals from the Pedra do Gavião syenogranite.

zircon crystals	Isotope ratios						1σ (%)	Age (Ma)					1σ (abs)	Rho	Th/U	Conc. (%)
	$^{206}Pb/^{204}Pb$	$^{207}Pb/^{206}Pb$	1σ (%)	$^{206}Pb/^{238}U$	1σ (%)	$^{207}Pb/^{235}U$		$^{207}Pb/^{206}Pb$	1σ (abs)	$^{206}Pb/^{238}U$	1σ (abs)	$^{207}Pb/^{235}U$				
03Z1	26048	0.08118	2.2	0.20453	1.4	2.2893	1.7	1225.8	43.1	1199.6	15.1	1209.0	12.3	0.77	0.19	97.87
35 Z22	38905	0.08051	0.7	0.20771	1.2	2.3058	1.4	1209.6	14.4	1216.6	13.1	1214.1	9.9	0.82	0.25	100.58
24 Z15	6227	0.08139	2.4	0.20624	3.9	2.3143	4.6	1230.8	46.2	1208.8	43.4	1216.7	32.5	0.84	0.34	98.21
21 Z12	44503	0.08065	0.8	0.20864	1.2	2.3202	1.4	1213.0	15.6	1221.6	13.2	1218.5	10.1	0.74	0.28	100.71
04 Z2	22802	0.08121	0.9	0.20999	1.1	2.3515	1.4	1226.6	16.9	1228.8	12.2	1228.0	9.9	0.75	0.13	100.18
06 Z4	21001	0.08109	1.3	0.21127	2.4	2.3621	2.7	1223.6	26.2	1235.6	26.7	1231.2	19.4	0.83	0.13	100.98
23 Z14	30657	0.10440	3.6	0.19949	2.5	2.8717	2.6	1703.9	64.8	1172.6	26.4	1374.5	19.5	0.94	0.42	68.82
29 Z18	23283	0.10878	2.9	0.24615	1.9	3.6919	2.1	1779.1	51.2	1418.6	24.8	1569.6	16.5	0.94	0.24	79.74
30 Z19	40184	0.10239	4.3	0.28692	2.9	4.0507	3.2	1667.9	78.2	1626.1	41.9	1644.4	25.8	0.89	0.21	97.49
10 Z6	20661	0.10929	2.0	0.28403	1.3	4.2803	1.5	1787.7	35.9	1611.6	18.1	1689.6	12.6	0.80	0.34	90.15
34 Z21	342823	0.10671	2.2	0.29881	1.5	4.3966	1.7	1744.0	40.2	1685.4	21.6	1711.7	13.8	0.84	0.27	96.64
33 Z20	56748	0.10761	2.1	0.30978	1.4	4.5965	1.6	1759.4	38.1	1739.6	21.6	1748.6	13.0	0.87	0.37	98.88
16 Z10	38681	0.10767	2.1	0.31225	1.3	4.6355	1.6	1760.4	37.8	1751.8	20.6	1755.7	13.3	0.80	0.27	99.51
05 Z3	43082	0.11064	0.7	0.32782	1.2	5.0008	1.4	1809.9	12.3	1827.8	19.2	1819.5	11.7	0.87	0.40	100.99
17 Z11	27175	0.11136	0.7	0.32596	1.1	5.0049	1.3	1821.8	13.2	1818.8	17.8	1820.2	11.4	0.79	0.31	99.84

Table 3. Whole-rock Sm–Nd isotopic data for the Pedra do Gavião syenogranite.

Sample	Sm (ppm)	Nd (ppm)	$^{147}Sm/^{144}Nd$	$^{143}Nd/^{144}Nd$	error (ppm)	εNd (0)	εNd (t=1218Ma)	T_{DM} (Ga)	f Sm/Nd
GH 11	25.30	152.07	0.1006	0.511691	10	-18.47	-3.54	1.81	-0.4885
GH 6	15.6	92.63	0.1018	0.511666	5	-18.97	-4.21	1.86	-0.4824
GH 4	18.73	115.89	0.0977	0.511691	6	-18.48	-3.09	1.76	-0.5033
GH 2	2.6	10.07	0.1560	0.511802	9	-16.30	-9.98	3.34	-0.2069

granites suites, which are exposed also in the southernmost portion of the Guyana shield, but in the Tapajós-Parima province (according to model suggested by Santos *et al.* 2000, 2006a), and mainly located within of the Waimiri-Atroari indigenous reserve area (Costi *et al.* 2000, CPRM 2006, Valério *et al.* 2009, Ferron *et al.* 2010). Due to the poor geological/geochronological knowledge of this region, it is likely that some granite, previously considered being Paleoproterozoic intrusions are in fact chronologically related to the Mesoproterozoic K'Mudku event (*e.g.* Santos *et al.* 2006b, 2009). Moreover, the field reconnaissance carried out during the present study has identified other granite bodies with textural features similar to the Pedra do Gavião syenogranite, suggesting the possible presence of an A-type granitic suite in the area that has not been properly studied.

Mesoproterozoic within-plate A-type granites, chronologically correlated to the K´Mudku period, have been recognized primarily in the southwestern margin of the Amazon craton and related to the Grenvillian-Sunsas orogenic belts (Priem *et al.* 1971, Sadowski & Bettencourt 1996, Dall'Agnol *et al.* 1999, Bettencourt *et al.* 1999, 2010, Geraldes *et al.* 2004, Cordani *et al.* 2010, Teixeira *et al.* 2010). The A-type Pedra do Gavião syenogranite has a post-collisional to within-plate geochemical signature, U-Pb crystallization age of 1218 Ma, inheritance ages between 1810 and 1780 Ma, which, together with the Sm-Nd isotopic data suggests partial melting of basement rocks of the Paleoproterozoic Cauaburi Complex. These results could require a revision of the geological/tectonic events responsible for this A-type magmatism during the Ectasian-Stenian period.

The origin of A-type granites has been the subject of much debate, especially in relation to their tectonic setting, emplacement mechanism and geochemical signature. A-type granites are commonly found in within-plate anorogenic settings or in the final stages of an orogenic event (*e.g.* Collins *et al.* 1982, Clemens *et al.* 1986, Whalen *et al.* 1987, Eby 1990, 1992, Dall'Agnol *et al.* 1994). The melting of the lower crust associated to mantle plume action or extensional thinning of the lithosphere associated with stress release-stages and generation of faults or mega-fractures are some of the tectonic models for A-type granites production (*e.g.* Windley 1991, Frost *et al.* 2001b, Goodge & Vervoort 2006, Martin *et al.* 2012).

There are geochronological correlations between crystallization ages from Pedra do Gavião (1218 Ma) and

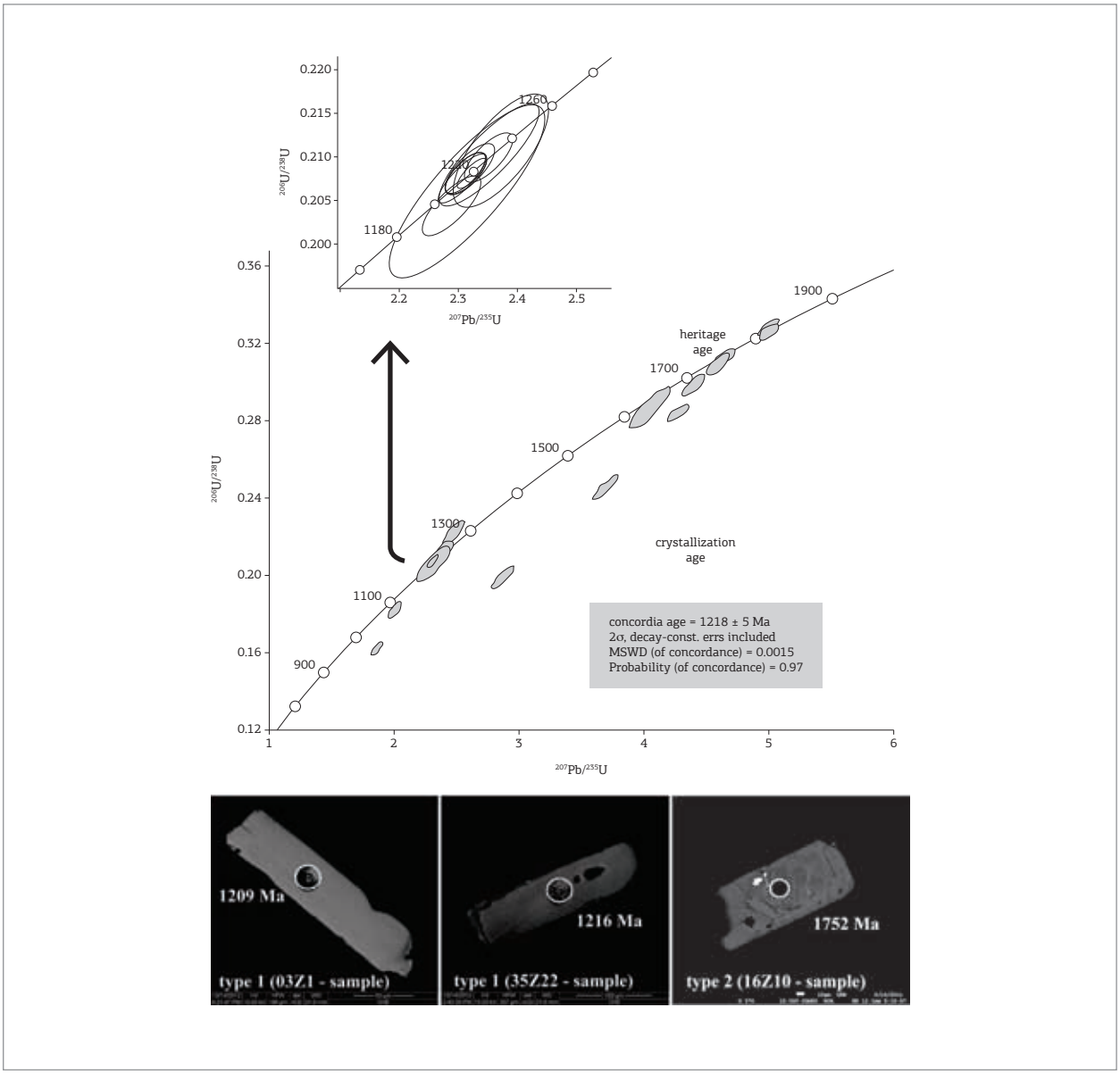

Figure 7. U–Pb concordia diagrams for zircon populations of rock sample GH-1 of the Pedra do Gavião granitic massif. BSE images of the zircon crystals (type 1 and type 2) with their ages are also shown. The white circle indicates the LA-MC-ICPMS spots position.

Samauma (1179 Ma) A-type magmatism and the time interval for K´Mudku deformational event (1490 – 1147 Ma). However, although there are geographical proximity also (Fig. 1B), the spatial relationship between K´Mudku event and A-type magma generation are not yet adequately clarified in the region.

On the other hand, K´Mudku event has been interpreted as an important structural distal effect from Grenvillian-Sunsas orogenies on an intracratonic tectonic setting (Teixeira 1978, Santos *et al.* 2000, 2006b, 2008, Cordani *et al.* 2010). Under this interpretation, it is reasonable to suggest that the Pedra do Gavião and Samauma A-type magmatism represents intracratonic distal activity at the end of the Grenvillian-Sunsas orogenies over central-north Amazonian craton. This magmatic activity very likely occurred related to the stress release along mega-fractures and with some degree of involvement in the final stages of the K´Mudku event. However, some questions still need to be answered (*e.g.* Santos *et al.* 2006b):

a) Did the development of the K'Mudku shear belt occurred during the Grenvillian-Sunsas orogenies or the K'Mudku shear belt represents the Mesoproterozoic reactivation during the Grenvillian-Sunsas orogenies of a trans-crustal

fault/lineament associated to an earlier collision zone of unknown age?; and

b) What is the tectonic framework conducive for the generation of A-type granites during the final stages of K´Mudku event?

To be able to answer these questions additional geological mapping work, mainly in the Waimiri-Atroari indigenous reserve area, together with new geochronological (U-Pb and Sm-Nd) data and seismic tomography investigations will be required.

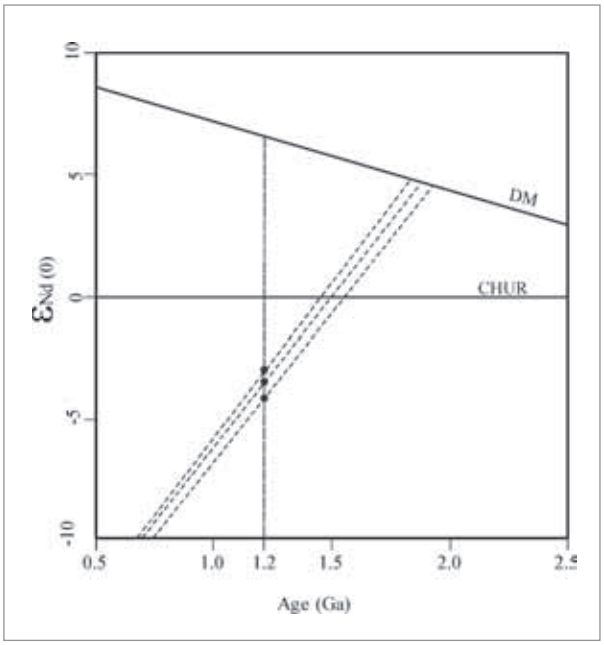

Figure 8. Nd evolution diagram for rock samples of the Pedra do Gavião syenogranite. Data for the sample GH-02 is not shown due to its strong fractionation.

CONCLUSION REMARKS

The Pedra do Gavião syenogranite (1218 ± 5 Ma) corresponds to a Mesoproterozoic (Ectasian-Stenian period) magmatic pulse with alkaline, metaluminous and A-type chemical characteristics. It is product of partial melting of the Paleoproterozoic basement rocks represented by the Cauaburi Complex (1810 – 1780 Ma), probably under reducing conditions and emplaced in a within-plate tectonic setting on an extensional mechanism.

These data demonstrate that the effects of the A-type magmatism associated to the end of the Grenvillian-Sunsas orogeny, reported primarily in the southwestern margin of the Amazon craton, may also be extended for the central-northern part of the Amazon craton. Probably the generation or emplacement mechanisms of A-type magma occurred with some degree of involvement in the final stages of the K´Mudku event. However, this tectonic framework conception still needs more geological and geophysical investigations. Therefore, these news data should instigate to the return of geological research in the region, as well as to debate on the tectonic evolution and A-type granites production during the Ectasian-Stenian period in the central-north Amazon craton.

ACKNOWLEDGEMENTS

This research was financially supported by Brazilian National Council of Technological and Scientific Development (CNPq) through of the CT-Amazonian project (MCTCNPq No. 575520/2008-6). We thank the technical staff of the isotope geology laboratories at the University of Brasília for their help. The authors are grateful to Dr. João Orestes S. Santos (University of Western Australia) for the useful review and critique applied on the first version this paper. Special thanks to Dr. Marcelo E. Almeida (CPRM – Brazilian Geological Service) and Dr. Marcio M. Pimentel (Geosciences Institute of the University of Brasília) for the review and suggestions that contributed to improving this paper. Finally, thanks to Dra. Leda M. B. Fraga (CPRM – Brazilian Geological Service) and anonymous reviewer for helpful comments that helped to improve the final text.

REFERENCES

Almeida M.E., Ferreira A.L., Pinheiro S.S. 2003. Associações graníticas do oeste do estado de Roraima, Domínio Parima, Escudo das Guianas, Brasil. *Géologie de la France*, **2-4:**135-159.

Almeida M.E., Macambira M.J.B., Reis N.J., Luzardo R., Pinheiro S.S. 2007. Geologia, geoquímica multielementar e isotópica (Sm-Nd) das rochas do embasamento do extremo oeste da Província Rio Negro, NW do Amazonas Brasil. *In*: SBG-NO, 10º Simpósio de Geologia da Amazônia, Porto Velho, *Anais*, **1**:26-29.

Almeida M.E., Macambira M.J.B., Santos, J.O.S., Nascimento R.S.C., Paquette J-L. 2013. Evolução crustal do noroeste do cráton Amazônico (Amazonas, Brasil) baseada em dados de campo, geoquímicos e geocronológicos. *In*: SBG-NO, 13º Simpósio de Geologia da Amazônia, Belém, CD-ROM.

Barron C.N. 1966. Notes on the stratigraphy of Guyana. In: 7nd Guyana Geological Conference, Paramaribo, *Proceedings* 6, pp. 1-28.

Bettencourt, J.S., Tosdal, R.M., Leite Jr., W.R., Payolla, B.L. 1999. Mesoproterozoic rapakivi granites of the Rondônia Tin Province, southwestern border of the Amazonianian craton, Brazil – I. Reconnaissance U-Pb geochronology and regional implications. *Precambrian Research*, **95**:41-67.

Bettencourt J.S., Leite Jr. W.B., Ruiz A.S., Matos R., Payolla B.L., Tosdal R.M. 2010. The Rondonian-San Ignacio Province in the SW Amazon craton: An overview. *Journal of South American Earth Science*, **29**:28-46.

Bosma W., Kroonenberg S.B., Maas K., De Roever E.W.F. 1983. Igneous and metamorphic complexes of the Guyana shield in Suriname. *Geologie en Mijnbouw, Netherlands Journal of Geosciences*, **62**(2):241-254.

Boynton W.V. 1984. Cosmogeochemistry of the rare earth elements: meteorite studies. *In*: Henderson, P. (Ed.), *Rare Earth Element Geochemistry*. Elsevier, pp. 63-114.

Bühn B., Pimentel M.M., Matteini M., Dantas E.L. 2009. High spatial resolution analysis of Pb and U isotopes for geochronology by laser ablation multi-collector inductively coupled plasma mass spectrometry (LA-MC-ICP-MS). *Anais da Academia Brasileira de Ciências*, **81**(1):1-16.

Clemens J.D., Holloway J.R., White A.J.R. 1986. Origin of an A-type granite: Experimental constraints. *American Mineralogist*, **71**:317-324.

Collins W.J., Beams S.D., White A.J.R., Chappell B.W. 1982. Nature and origin of A-type granites. *Contributions to Mineralogy and Petrology*, **80**:189-200.

Cordani U.G., Fraga L.M., Tassinari C.C.G., Brito-Neves B.B. 2010. On the origin and tectonic significance of the intra-plate events of Grenvillian-type age in South America: A discussion. *Journal of South American Earth Science*, **29**:143-159.

Costi H.T., Dall´Agnol R., Moura C.A.V. 2000. Geology and Pb-Pb geochronology of Paleoproterozoic volcanic and granitic rocks of the Pitinga Province, northern Brazil. *International Geology Reviews*, **42**:832-849.

Companhia de Pesquisa de Recursos Minerais (CPRM). 1999. Projeto Roraima Central, Folhas NA.20-X-B e NA.20-X-D (inteiras), NA.20-X-A, NA.20-X-C, NA.21-V-A e NA.21-V-C (parciais). MME-CPRM, Brasília, *Programa de Levantamentos Geológicos Básicos do Brasil*, CR-ROM.

Companhia de Pesquisa de Recursos Minerais (CPRM). 2006. Geologia e recursos minerais do Estado do Amazonas. MME/CPRM/CIAMA, *Programa de Geologia do Brasil (mapas geológicos estaduais, escala 1:1.000.000)*, Manaus, Texto Explicativo, 144 p., CR-ROM.

Dall'Agnol R., Lafon J.M., Macambira M.J.B. 1994. Proterozoic anorogenic magmatism in the Central Amazonian Province, Amazonian Craton: geochronological, petrological and geochemical aspects. *Mineralogy and Petrology*, **50**(1-3):113-138.

Dall'Agnol R., Costi H.T., Leite A.A.S., Magalhães M.S., Teixeira N.P. 1999. Rapakivi granites from Brazil and adjacent areas. *Precambrian Research*, **95**(1):9-39.

Dall'Agnol R. & Oliveira D.C. 2007. Oxidized, magnetite-series, rapakivi-type granites of Carajás, Brazil: Implications for classification and petrogenesis of A-type granites. *Lithos*, **93**(3):215-233.

De Paolo, D. 1981. Neodymium isotopes in the Colorado Front Range and crust-mantle evolution in the Proterozoic. *Nature*, **291**:193-196.

Eby, G.N. 1990. The A-type granitoids: A review of their occurrence and chemical characteristics and speculations on their petrogenesis. *Lithos*, **26**:115-134.

Eby G.N. 1992. Chemical subdivisions of A-type granitoids: Petrogenesis and tectonic implications. *Geology*, **20**:614-644.

Ferron, J. M. T.M., Bastos Neto, A. C., Lima, E. F., Nardi, L. V.S., Costi, H.T., Pierosan, R., Prado, M. 2010. Petrology, geochemistry, and geochronology of Paleoproterozoic volcanic and granitic rocks (1.89–1.88 Ga) of the Pitinga Province, Amazon craton, Brazil. *Journal of South American Earth Sciences*, **29**:483-497.

Fraga L.M.B. & Reis N.J. 1996. A Reativação do Cinturão de Cisalhamento Guiana Central durante o Episódio K'Mudku. *In*: SBG, 39º Congresso Brasileiro de Geologia, Salvador, *Anais*, v. 1, p. 424-426.

Fraga L.M.B. 2002. *A associação Anortosito-Mangerito-Granito Rapakivi (AMG) do cinturão Guiana Central, Roraima e suas encaixantes paleoproterozóicas: evolução estrutural, geocronologia e petrologia*. PhD Thesis, Instituto de Geociências, Universidade Federal do Pará, Belém, 386 p.

Fraga L.M., Dall'Agnol R., Costa J.B.S., Macambira M.J.B. 2009. The Mesoproterozoic Mucajaí anorthosite-mangerite-rapakivi granite complex, Amazonian Craton, Brazil. *The Canadian Mineralogist*, **47**:1469-1492.

Frost B.R., Barnes C.G., Collins W.J., Arculus R.J., Ellis D.J., Frost C.D. 2001a. A geochemical classification for granitic rocks. *Journal of Petrology*, **42**(11):2033-2048.

Frost C.D., Bell J.M., Frost B.R., Chamberlain K.R. 2001b. Crustal growth by magmatic underplating: Isotopic evidence from the northern Sherman batholith. *Geology*, **29**(6):515-518.

Gaudette H.E., Olszewski W.J. Jr., Santos J.O.S. 1996. Geochronology of Precambriam rocks from the northern part of Guiana Shield, State of Roraima, Brazil. *Journal of South American Earth Sciences*, **9**:183-195.

Geraldes M.C., Teixeira W., Heilbron M. 2004. Lithospheric versus asthenospheric source of the SW Amazonian craton A-types granites: the role of the Paleo- and Mesoproterozoic accretionary belts for their coeval continental suítes. *Episodes*, **27**(3):185-189.

Gibbs A.K. & Barron C.N. 1993. *The Geology of the Guiana Shield*. New York, Oxford, Oxford University Press, Claredon Press. 245 p.

Gioia S.M.L. & Pimentel M.M. 2000. The Sm–Nd isotopic method in the Geochronology Laboratory of the University of Brasília. *Anais da Academia Brasileira de Ciências*, **72**(2):219-245.

Goldstein S.L., O'Nions R.K., Hamilton P.J. 1984. A Sm–Nd isotopic study of atmospheric dusts and particulates form major river systems. *Earth and Planetary Science Letters*, **70**:221-236.

Goodge J.W. & Vervoort J.D. 2006. Origin of Mesoproterozoic A-type granites in Laurentia: Hf isotope evidence. *Earth and Planetary Science Letters*, **243**:711-731.

Lima M.I.C. & Pires J.L. 1985. Geologia da região do Alto Rio Negro - AM. *In*: SBG-NO, 2º Simpósio de Geologia da Amazônia, Belém, *Boletim*, **1**:140-154.

Ludwig K.R. 2003. *User's Manual for Isoplot/Ex, Version 3.0, a geochronological toolkit for Microsoft Excel*. Berkeley Geochronology Center, Special Publication, v. 4, Berkeley, Geochronology Center.

Maas E.C.A.S. & Souza V.S. 2009. Maciços graníticos como rochas ornamentais na região nordeste do Estado do Amazonas: uma perspectiva de investimento para a cidade de Manaus. *Revista Escola de Minas*, **62**(3):343-348.

Maniar P.D. & Piccoli P.M. 1989. Tectonic discrimination of granitoids. *Geological Society of America Bulletin*, **101**(5):635-643.

Martin R.F., Sokolov M., Magaji S.S. 2012. Punctuated anorogenic magmatism. *Lithos*, **152**:132-140.

Montalvão R.G.M., Muniz C.M., Issler R.S., Dall´Agnol R., Lima M.I.C., Fernandes P.E.C.A., Silva G.G. 1975. *Geologia da Folha NA.20-Boa Vista e parte das folhas NA.21-Tumucumaque, NB.20-Roraima e NB.21*. Projeto RADAMBRASIL, DNPM, Rio de Janeiro, cap. I – Geologia. (Levantamentos de Recursos Naturais, vol. 8).

Pearce J.A., Harris N.B.W., Tindle A.G. 1984. Trace element discrimination diagrams for the tectonic interpretation of granitic rocks. *Journal of Petrology*, **25**:956-983.

Priem H.N.A., Boelrijk N.A.I.M., Hebeda E.H., Verdurmen E.A.Th., Verschure R.H., Bom E.H. 1971. Granitic complexes and associated tin mineralizations of "Grenville"age in Rondônia, western Brazil. *Geological Society of America Bulletin*, **82**(4):1095-1102.

Rollinson H. 1993. *Using geochemical data: evaluation, presentation, interpretation*. London, Longman Scientific & Technical, 352 p.

Sadowski G.R. & Bettencourt J.S. 1996. Mesoproterozoic tectonic correlations between eastern Laurentia and the western border of the Amazon Craton. *Precambrian Research*, **76**:213-227.

Santos J.O.S., Souza M.M., Prazeres W.V., Silva L.S., Barreto E.L., Pessoa M.R. 1974. *Projeto Norte da Amazônia, Domínio Baixo Rio Negro, geologia da folha SA.20-X. CPRM-DNPM*, Manaus, volume IIA.

Santos J.O.S., Hartmann L.A., Gaudette H.E., Groves D.I., McNaughton N.J., Fletcher I.R. 2000. A New understand of the provinces of the Amazon Craton based on integration of field mapping and U-Pb and Sm-Nd geochronology. *Gondwana Research*, **3**(4):453-488.

Santos J.O.S. 2003. Geotectônica dos Escudos das Guianas e Brasil-Central. *In*: Bizzi L.A., Schobbenhaus C., Vidotti R.M., Gonçalves J.H. (eds.) *Geologia, Tectônica e Recusrsos Minerais do Brasil (texto, mapas & SIG)*. Brasília, Serviço Geológico do Brasil – CPRM/MME, p.169-226.

Santos J.O.S., Hartmann L.A., Faria M.S.G., Riker S.R., Souza M.M., Almeida M.E., McNaughton N.J., 2006a. A compartimentação do Cráton Amazonas em províncias: avanços ocorridos no período 2000-2006. *In*: SBG-NO, 9º Simpósio de Geologia da Amazônia, Belém, CD-ROM.

Santos J.O.S., Faria M.S.G., Riker S.R., Souza M.M., Hartmann L.A., Almeida M.E., McNaughton N.J., Fletcher I.R. 2006b. A faixa colisional K'mudku (idade grenvilliana) no norte do cráton Amazonas: reflexo intracontinental do orógeno Sunsás na margem ocidental do cráton. *In*: SBG-NO, 9º Simpósio de Geologia da Amazônia, Belém, CD-ROM.

Santos, J.O.S., Rizzotto, G.J., Potter, P.E., McNaughton, N.J., Matos, R.S., Hartmann, L.A., Chemale Jr., F., Quadros, M.E.S. 2008. Age and authochtonous evolution of the Sunsás Orogen in West Amazon Craton based on mapping and U-Pb geochronology. *Precambrian Research*, **165**:120-152.

Santos J.O.S., McNaughton, N.J., Almeida, M.E. 2009. Magmatismo de idade Sunsás no centro-norte do cráton Amazonas. *In*: SBG-NO, 11º Simpósio de Geologia da Amazônia, Manaus, CD-ROM.

Shand S.J. 1943. The eruptive rocks. New York, John Wiley ed., 2nd, 444 p.

Souza A.G.H., Souza V.S., Dantas E.L., Valério C.S., Laux J.H., Silva A.J.M., Ferreira J.R., 2006. Pedra do Gavião massif: record of the 1.23 Ga A-type magmatism in the southern Guyana shield. *In*: Symposium on Magmatism, Crustal Evolution, and Metallogenesis of the Amazon craton (Abstract Volume and Field Trips Guide). PRONEX/IGCP (Project 510)/UFPA/SBG-NO, Belém, Brazil, CD-ROM. p.73.

Streckeisen A. 1976. To each plutonic rock its proper name. *Earth Science Reviews*, **12**(1):1-33.

Tassinari C.C.G. & Macambira M.J.B. 1999. Geochronological provinces of the Amazon craton. *Episodes*, **22**(3):174-182.

Tassinari C.C.G., Bettencourt J.S., Geraldes M.C., Macambira M.J.B., Lafon J.M. 2000. The Amazon craton. *In*: UG Cordani, EJ Milani, A Thomaz Filho, DA Campos (Edit.). *Tectonic Evolution of South America*. 31st International Geological Congress, Rio de Janeiro, Brazil, p. 41-95.

Teixeira W. 1978. Significação tectônica do magmatismo anorogênico pré-Cambriano básico e alcalino na região Amazônica. *In*: SBG, 30º Congresso Brasileiro de Geologia, *Anais*, Recife **1**:477-490.

Teixeira W., Geraldes M. C., Matos R., Ruiz A. S., Saes G., Vargas-Mattos G. 2010. A review of the tectonic evolution of the Sunsás belt, SW Amazon craton. *Journal of South America Earth Science*, **29**:47-60.

Thompson R.N. 1982. Magmatism of the British Tertiary volcanic province. *Scottish Journal of Geology*, **18**:49-107.

Valério C.S., Souza V.S. Macambira M.J.B. 2009. The 1.90–1.88 Ga magmatism in the southernmost Guyana Shield, Amazonas, Brazil: Geology, geochemistry, zircon geochronology, and tectonic implications. *Journal of South American Earth Sciences*, **28**:304-320.

Whalen J.B., Currie K.L., Chappell B. 1987. A-type granites: Geochemical characteristics, discrimination and petrogenesis. *Contributions to Mineralogy and Petrology*, **95**:407-419.

Windley B.F. 1991. Early Proterozoic collision tectonics, and rapakivi granites as intrusions in an extensional trust-thickened crust: the Ketilidian orogen, south Greenland. *Tectonophysics*, **195**:1-10.

Arquivo digital disponível on-line no site www.sbgeo.org.br